MOLECULAR IMAGING AND BIOLOGY

Mol Imaging Biol (2019) 21:401–409
DOI: 10.1007/s11307-018-1236-5

Published Online: 12 July 2018

REVIEW ARTICLE

The Complexity and Fractal Geometry of Nuclear Medicine Images

Fabio Grizzi,[1,2] Angelo Castello,[3] Dorina Qehajaj,[1] Carlo Russo,[4] Egesta Lopci[3]

[1]*Department of Immunology and Inflammation, Humanitas Clinical and Research Hospital, Via Manzoni 56 - Rozzano, 20089, Milan, Italy*
[2]*Humanitas University, Via Rita Levi Montalcini, Pieve Emanuele, 20090, Milan, Italy*
[3]*Department of Nuclear Medicine, Humanitas Clinical and Research Hospital, Via Manzoni 56 - Rozzano, 20089, Milan, Italy*
[4]*"Michele Rodriguez" Foundation, Via Ludovico di Breme, 79, 20156, Milan, Italy*

Abstract

Irregularity in shape and behavior is the main feature of every anatomical system, including human organs, tissues, cells, and sub-cellular entities. It has been shown that this property cannot be quantified by means of the classical Euclidean geometry, which is only able to describe regular geometrical objects. In contrast, fractal geometry has been widely applied in several scientific fields. This rapid growth has also produced substantial insights in the biomedical imaging. Consequently, particular attention has been given to the identification of pathognomonic patterns of "shape" in anatomical entities and their changes from natural to pathological states. Despite the advantages of fractal mathematics and several studies demonstrating its applicability to oncological research, many researchers and clinicians remain unaware of its potential. Therefore, this review aims to summarize the complexity and fractal geometry of nuclear medicine images.

Key words: Fractals, Geometry, Complexity, Anatomy, Nuclear medicine

The Complexity of Human Beings

Organisms are complex systems, being composed of many interacting parts, including molecules, cells, tissues, organs, and systems or apparatuses [1, 2]. The more those parts depend on each other, the more integrated those parts are thought to be. In this way, "integration" may be considered an emergent property of complexity. Simon Alexander Herbert (1916–2001) stated "By a hierarchic system or hierarchy, I mean a system that is composed of interrelated sub-systems, each of the latter being, in turn, hierarchic in structure until we reach some lowest level of elementary subsystem" [3]. Ludwig von Bertalanffy (1901–1972) well explained the term "complexity" as one made up of a large number of parts that interact in a non-simple way [4–6]. The need for a new way of classifying complex natural as well as pathological anatomic forms has prompted an increasing number of researchers to adopt the "fractal geometry" [7–10], which appears a more suitable tool in this context [11–16].

Review Criteria

A literature review of PubMed/Medline was performed using the following sets of keywords: "Fractal" AND "Nuclear Medicine." The search included articles published in English online through February 28, 2018. The two keyword sets yielded 138 publications. After excluding publications that primarily unfit the aim of the research, the remaining 22 publications were reviewed and discussed.

Euclidean *Versus* Fractal Geometry

Unlike Euclidean geometry, fractal geometry is able to describe with higher approximation complex natural structures and biological dynamic processes [17–19]. A fractal

Correspondence to: Egesta Lopci; *e-mail:* egesta.lopci@gmail.com

structure can be defined as having a characteristic form that remains constant over a defined range of scales. Similarly, a process is fractal if a variable undergoes characteristic changes that are similar regardless of the time interval over which the observations are made [20]. The concept of fractal geometry was developed by Benoit B. Mandelbrot (1924–2010), based on previous works by Jules Henri Poincaré (1854–1912), Georg Ferdinand Ludwig Philipp Cantor (1845–1918), and Lewis Fry Richardson (1881–1953). Mandelbrot first adopted the term "fractal" in his book entitled "Les Objets Fractals: Forme, Hasard et Dimension" and subsequently in "The Fractal Geometry of Nature." He came forward with a universal mathematical code for interpreting the multifarious world of natural forms. As stated by the mathematician Michael Fielding Barnsley (1946–), we can find "fractals everywhere." This statement is supported by the recognized importance of the "rough" shape as geometrical property of natural structures and anatomical systems, capable of influencing behavior and relationship with the surrounding environment [21]. In this context, one spatial scale and typical Euclidean geometry result are not sufficient for describing natural objects, as stated by Mandelbrot [22]. Based on these assumptions, the fractal dimension, also called non-integer dimension, has been introduced as an estimator of the space-filling properties of irregularly shaped objects and continually applied into the life sciences in biology and medicine [23–26].

The Bases of Fractal Geometry

The word "fractal", derived by the Latin *fractus* meaning "broken," was first coined in 1975 by Mandelbrot to describe complex patterns that were self-similar across infinite scales [17]. Namely, fractal objects are detailed or fragmented geometric forms that can be segmented into smaller parts, each representing a miniature or rough copy of the entire object. Every element of these reduced copies can be subsequently divided into smaller parts, and then these divided into more smaller elements, and so on to the infinite, providing substructures all characterized by exact, quasi, or statistical self-similarity to the whole. As shown by Mandelbrot, the simplest principle of fractals is the so-called recursive iteration. For example, the Mandelbrot set arises from the simple $Z = Z2 + C$ recursive algorithm (Fig. 1a). Other examples include the Julia set originally proposed by the French mathematician Gaston Julia (1893–1978) (Fig. 1b).

The classic examples of geometrically self-similar objects are the "snowflake" and the "curve" (Fig. 1c, d), described by Niels Fabian Helge von Koch (1870–1924), or the "Sierpinski triangle" (Fig. 1e), described by the

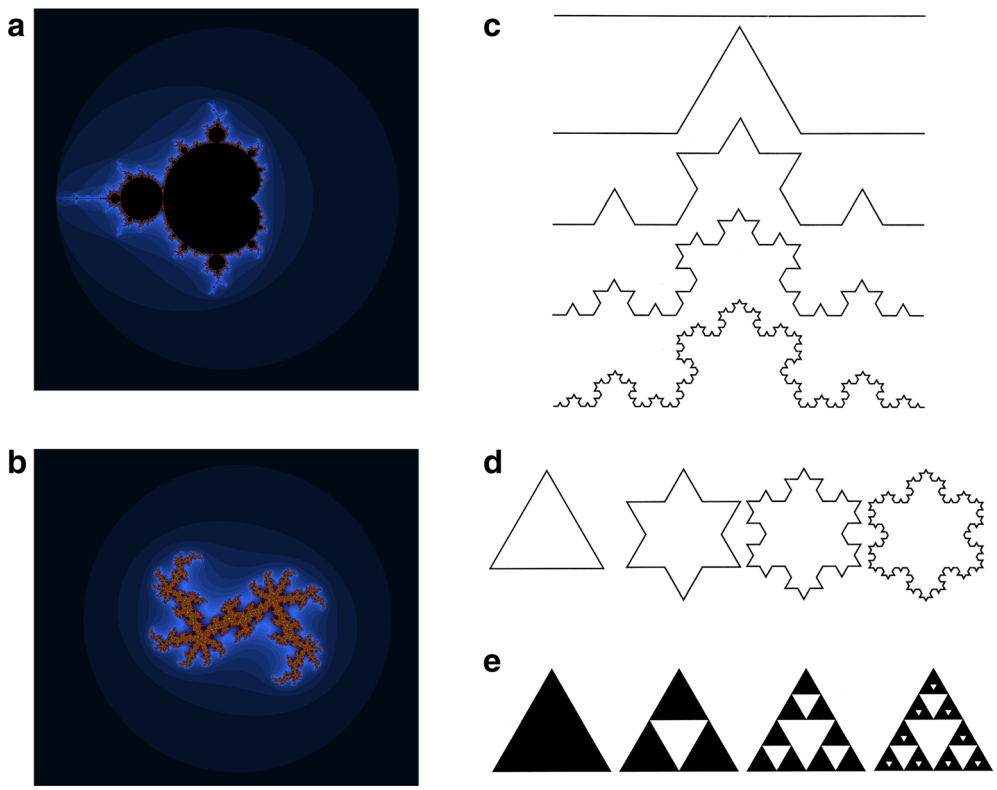

Fig. 1. Prototypical examples of geometrical fractals. **a** Mandelbrot set arising from the simple $Z = Z^2 + c$ recursive algorithm, where any new Z complex number is generated by its predecessor. **b** Julia set originally proposed by the French mathematician Gaston Julia. The classic examples of geometrically self-similar objects are **c** the "curve" from Niels Fabian Helge von Koch and **d** the "snowflake". **e** Another geometrically self-similar figure is the "Sierpinski triangle."

Polish mathematician Waclaw Sierpinski (1882–1969). On the other hand, statistical self-similarity also called "self-affinity" concerns biological objects. Anatomic systems are rarely identical copies of the whole system. Self-similar structures in human anatomy, anyhow, can be depicted in the circulatory system, in the biliary and bronchial trees, in the mammary ductal system, in the neuronal system, in cell membrane, *etc.* [11, 21, 27–39] (Fig. 2). What all these anatomical examples of fractal objects have in common are four properties: (a) they have an irregular shape, (b) their structures are characterized by self-similarity, (c) their geometrical analysis can be done with non-integer, fractal dimension, and lastly (d) the measurement of their properties depends on the scale they are studied.

Measurement of Fractal Properties

A fundamental concept for the evaluation of geometric objects is that of dimension. Two main definitions of dimension have been proposed. The first, named "topological dimension," assigns an integer number to every point in Euclidean space, indicated with the symbol E3, and attributes a dimension of 0 to the "point," dimension 1 to the "straight line," dimension 2 to the "plain surface," and dimension 3 to the "three-dimensional figure" [26]. The second definition of dimension attributes a real number to every natural object in E3, lying between the topological dimension and 3. Mandelbrot indicates the first with the symbol D_γ and the second with the symbol D. For all Euclidean figures, D_γ and D are coincident ($D_\gamma = D$), but this is not valid for all fractal objects because $D > D_\gamma$. As suggested by Mandelbrot, it is possible to determine irregularly shaped objects through the covering procedure of the topological space of the object being measured. Algorithms to estimate the fractal dimension have been previously explained by Di Ieva et al. [4] and are illustrated in Fig. 3a–b.

Fractal Geometry in Oncology

In biology, we are often faced with the complexity of cellular systems due to the presence of multiple different structures, such as cell membranes, vascular structures, or neurons. The same goes for pathological tissues, *i.e.*, tumors, characterized by variations on cell death, metabolic activity, and proliferation. As a consequence, all attempts to describe such natural complexity graphically by conventional geometry have failed and still remain challenging [40]. As tumor outlines are fractals, they can be characterized by a proper non-integer dimension, which exceeds the integer Euclidean dimension. Kikuchi et al. [41] showed that the surface of endometrioid endometrial adenocarcinoma has a fractal structure, and the mean fractal dimension may differ according to histologic grades. Additionally, in the study of Lee et al. [42], fractal dimension was able to differentiate between squamous cell carcinoma and adenocarcinoma of the lung, this latter characterized by lower fractal dimensions. Vasiljevic et al. [43] showed that parameters of multifractal analysis were significantly different among three types groups of malignancy that produce

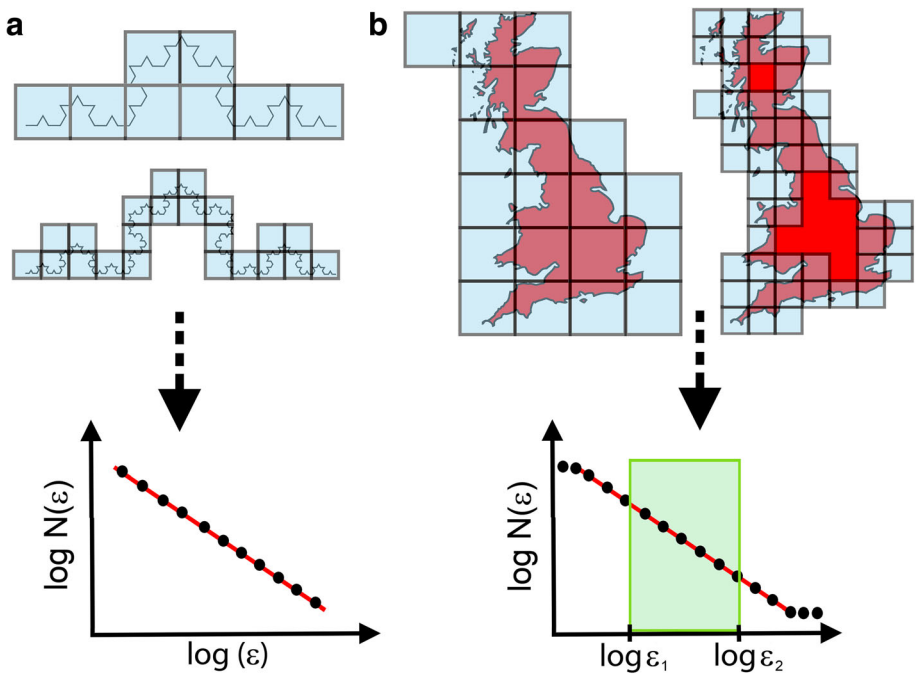

Fig. 2. Prototypical examples of natural fractal structures. **a** The ramified organization of a vegetable tree, **b** a cloud with its irregular edges in continuous movement, and the counterpart anatomical fractal systems including the **c** retinal vascular tree and **d** the irregularly shaped collagen fibers abnormally deposited during a chronic reparative process.

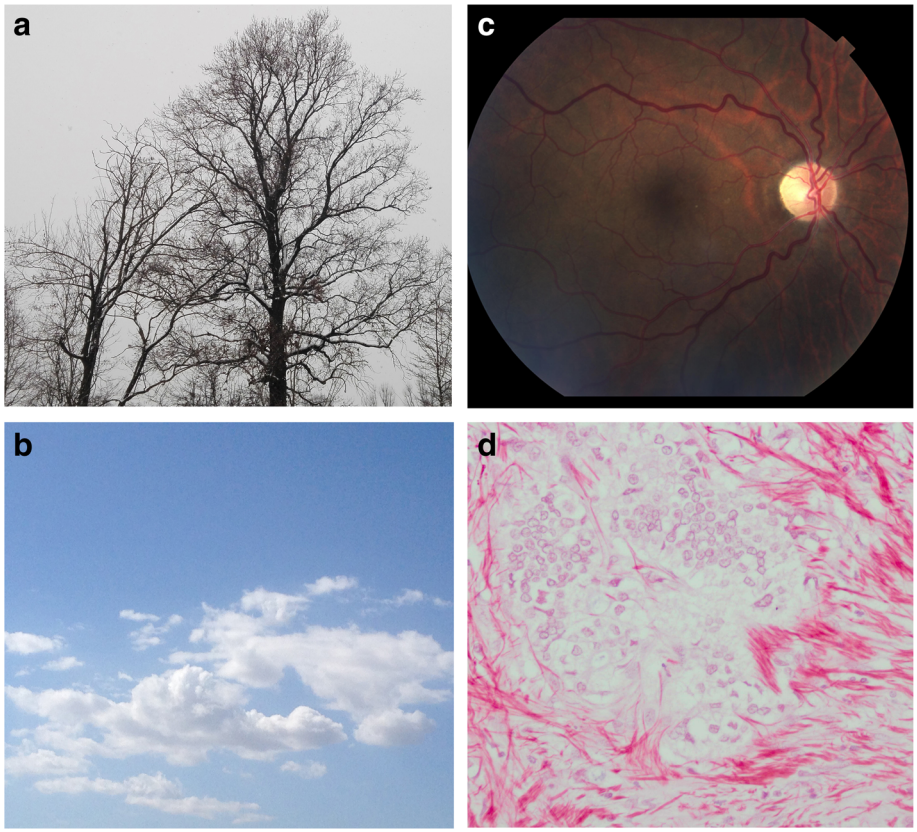

Fig. 3. The most widely used in the biomedical sciences is called the "box-counting method.". **a** The "box-counting" dimension is an estimator of the space-filling properties of natural objects in two-dimensions and three-dimensions. The Koch curve represents an ideal model to examine the characteristic of the scale-dependent length of fractal structures. By looking at these pictures, it is easy to see that a line in the Koch curve breaks up into four smaller pieces. Each of these pieces are 1/3 the length of the original. Therefore, *N* is equal to four and *S* is equal to three, which gives us a fractal dimension of 1.231. **b** Because the zero limit cannot be applied to natural objects, the dimension is the slope of the graph in a fixed range of side lengths (ε_1–ε_2) empirically evaluated. This can lead to the derivation of resolution correction factors, which permit measurements obtained at any magnification to be converted to estimates at critical magnification. These findings may explain the potential discrepancy in the estimates of the outline or surface of anatomical shapes.

bone metastases (*i.e.*, renal, breast, and lung carcinoma), postulating a potential application of this new analysis for detecting primary tumor in patients with metastatic cancer of unknown origin. In 2010, Di Ieva et al. [44] have evaluated the microvascular network complexity of six cases of human glioblastoma multiforme estimating the box-counting surface fractal dimension on CD34 immunostained specimens. The different fractal dimension values observed showed that the same histological category of brain tumor had different microvascular network architectures.

In the last years, several papers have been also published comparing the modifications in chromatin fractal dimension between cancer and their natural counterpart in routinely stained histological or cytological preparations. Overall, they have shown that fractal dimension of chromatin rises in different tumors during the phase from dysplasia to cancer, from initial cancer to metastatic stages or in patients with poor prognosis [45–51].

Fractal Geometry in Oncology Nuclear Medicine

Positron emission tomography using the radioactive biomarker 2-deoxy-2[^{18}F]fluoro-D-glucose ([^{18}F]FDG) has gained widespread use in oncology due to the relatively high accuracy in the staging, differential diagnosis, and therapy monitoring. Functional information, such as metabolic tumor activity expressed by standardized uptake values (*i.e.*, SUVmax, SUVmean), could be used to detect regional variation within the tumors [50–53]. However, these parameters still define tumor heterogeneity in terms more descriptive, at most semi-quantitative, rather than quantitative. Thus, it is rational using fractal analysis as a quantitative tool for positron emission tomography (PET) images in order to detect structural heterogeneity of tumor and monitor the disease evolution and the response to different treatment plans [54].

Recently, Michallek and Dewey [55] have provided a systematic review on fractal analysis applied to radiological

and nuclear medicine tissue on perfusion imaging of tumors, lung, myocardium, kidney, skeletal muscle, and cerebral diseases. From the review emerged that fractal analysis can be successfully performed and it is a suitable method for quantifying perfusion heterogeneity. Nevertheless, the studies monitoring tumor response to treatment have showed limited significance, with only one study demonstrating successfully correlation between treatment response and fractal analysis.

As mentioned above, Di Ieva et al. [44] showed that the same histological category of brain tumors had different microvascular network architectures. Additionally, a significant positive correlation between the microvascular fractal dimension and [^{11}C]methionine ([^{11}C]MET) uptake was found. Their preliminary findings indicated that microvascular fractal dimension can be a useful parameter to objectively describe and quantify the geometrical complexity of the microangioarchitecture in glioblastoma multiforme.

The lung, due to its hierarchical branching structure, is one of the most recognized examples of biological fractal system (Fig. 4). Miwa et al. [56] determined whether fractal analysis of morphological complexity and intratumoral heterogeneity of [^{18}F]FDG uptake can help to differentiate malignant from benign pulmonary nodules. The authors included in their study 54 patients with suspected non-small cell lung cancer who were examined by [^{18}F]FDG PET/x-ray computed tomography (CT). The density fractal dimension of intratumoral heterogeneity of FDG uptake was lower for malignant than benign pulmonary nodules. The authors stated that the combination of glucose metabolism (SUVmax) and heterogeneity of [^{18}F]FDG uptake by fractal analysis is complementary for differential diagnoses and improves diagnostic accuracy. Dimitrakopoulou-Strauss et al. [57], using a two-tissue compartment model and a non-compartment model based on the fractal dimension, compared the kinetic parameters of [^{18}F]FDG and [^{68}Ga]DOTATOC in patients with non-small cell lung cancer (NSCLC). Such comparison revealed a significant correlation for fractal dimension of the two tracers ($r = 0.764$, $p = 0.017$), which could reflect a heterogeneous time-dependent distribution of both tracers in the lung tumors. Moreover, Dimitrakopoulou-Strauss et al. [58] compared the fractal dimensions of the time–activity data for 6-[^{18}F]fluoro-L-dopa ([^{18}F]FDOPA), [^{18}F]FDG, and [^{15}O]water in a series of metastatic melanoma lesions. They did not observe significant differences for the median values of the fractal dimension between the tracers within a tumor VOI. In the same context of metastatic melanoma, Breki et al. [59] have applied fractal/multifractal analysis to assess tumor response in 31 patients treated with ipilimumab. They found that fractal dimension was lower in patients with progressive disease, suggesting hierarchical expansion of low dimensionality by malignant lesions, whereas in cases of successful therapy, the lesions cease to attract the tracer, which diffuses in all parts of the body.

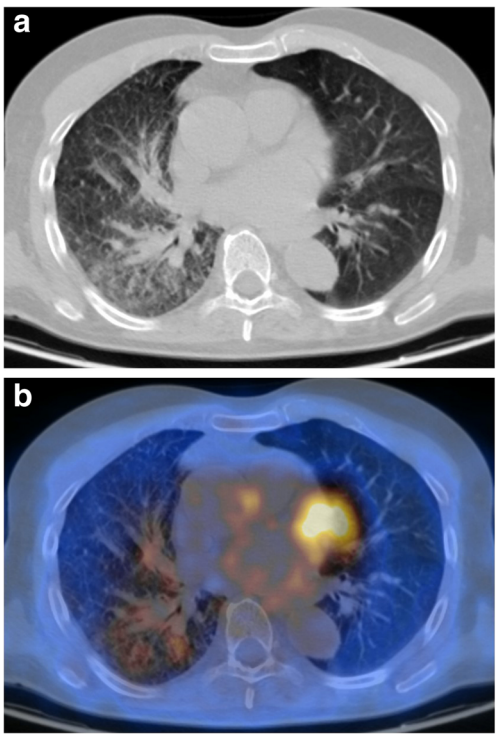

Fig. 4. The practice of nuclear medicine involves looking at an image (*i.e.*, visual perception) and interpreting what is seen (*i.e.*, cognition). Experience gives the perceptual and cognitive skills to know what information to look for and how to interpret that information based on the accumulation and integration of information processed from previous encounters with the same types of images. Although the basic anatomy, **a** the CT bronchial tree or **b** the representative fused PET/CT image, is the same from image to image, the degree of natural dissimilarity in both normal and pathological anatomical structures is high.

The same study group [60] also evaluated fractal analysis to characterize dynamic [^{18}F]FDG uptake in patients with sarcoma. Interestingly, they found that SUV and the fractal dimension were helpful for the differentiation of the lipoma and scar tissue from advanced sarcoma stages (grades III–IV). Afterwards, Okazumi et al. [61] reported that the fractal analysis on dynamic [^{18}F]FDG PET/CT study was useful for predicting the grade and prognosis of soft tissue sarcomas.

Additionally, another paper from Dimitrakopoulou-Strauss et al. [62] aimed to compare different dynamic [^{18}F]FDG PET quantification methods to predict survival in a cohort of patients with metastatic colorectal cancer under chemotherapy. The results showed that patients with either high baseline SUV (6.0) or high baseline fractal dimension (1.35) were associated with poor prognosis and short survival.

Similarly, the same group [63] compared dynamic PET parameters of [^{18}F]FDG and [^{68}Ga]DOTATOC in patients with metastatic neuroendocrine tumors, in whom [^{90}Y]DOTATOC therapy was planned. However, they did not find any significant correlation between fractal dimensions for [^{18}F]FDG and the corresponding [^{68}Ga]DOTATOC values.

Sachpekidis et al. [64] studied the pharmacokinetics and distribution of the Ga-68 prostate-specific membrane antigen (PSMA) PET/CT in patients with recurrent prostate cancer. Fractal dimension values were higher in tumor-related lesions than in reference tissue and in the osseous metastatic lesions than primary tumors and lymph node metastases. Additionally, they found a significant correlation between fractal dimension and SUVmean ($r = 0.93$), fractal dimension and SUVmax ($r = 0.87$), and fractal dimension and influx rate ($r = 0.77$). Recently, the same group further confirmed their results [65].

The same group investigated static and dynamic [^{18}F]FDG and [^{18}F]sodium fluoride ([^{18}F]NaF) PET/CT in treatment response assessment in multiple myeloma patients. Quantitative analysis of dynamic PET/CT for both tracers revealed that the patients who responded to therapy had a

Table 1.. Overview of reports of fractal geometry in nuclear medicine

Study	Radiotracer	Tissue/organ	No. of patients	Comments
Oncology				
Di Ieva et al. [44]	[^{11}C]MET	Glioblastoma multiforme	6	Significant correlation between the microvascular FD and the uptake of [^{11}C]MET
Miwa et al. [56]	[^{18}F]FDG	Pulmonary nodules	54	m-FD and d-FD differ between malignant and benign pulmonary nodules.
Dimitrakopoulou-Strauss et al. [57]	[^{18}F]FDG, [^{68}Ga]DOTATOC	NSCLC	9	Significant correlation of the FD of [^{18}F]FDG and [^{68}Ga]DOTATOC
Dimitrakopoulou-Strauss et al. [58]	[^{18}F]FDG, [^{18}F]DOPA, [^{15}O]water	Metastatic melanoma	11	No significant heterogeneous distribution among the tracers
Breki et al. [59]	[^{18}F]FDG	Metastatic melanoma	31	FD decreases with the deterioration of the patient's therapeutic outcome condition.
Dimitrakopoulou-Strauss et al. [60]	[^{18}F]FDG	Sarcoma	56	FD distinguishes advanced sarcoma stages from benign lesions.
Okazumi et al. [61]	[^{18}F]FDG	Sarcoma	117	FD is a useful parameter for malignant lesions at the diagnosis, for histological grading, and for prognosis.
Dimitrakopoulou-Strauss et al. [62]	[^{18}F]FDG	Metastatic colorectal cancer	25	FD > 1.35 associated with shorter survival.
Koukouraki et al. [63]	[^{18}F]FDG, [^{68}Ga]DOTATOC	Metastatic NETs	15	No significant correlation between the tracers
Sachpekidis et al. [64]	[^{68}Ga]PSMA	Prostate cancer	24	FD values from cancer lesions significantly higher than normal prostate tissue
Sachpekidis et al. 65]	[^{68}Ga]PSMA	Prostate cancer	140	FD correlates with the level of tracer uptake and influx rate.
Sachpekidis et al. [66]	[^{18}F]FDG, [^{18}F]NaF	Myeloma	34	Decrease of FD values for patients who respond to the therapy
Dimitrakopoulou-Strauss et al. [67]	[^{18}F]FDG	Myeloma	19	Significant reduction of FD after chemotherapy
Ben Bouallègue et al. [68]	[^{18}F]FDG	Lymphoma	57	Low 2D and 3D fractal dimensions associated with complete metabolic response
Tochigi et al. [69]	[^{18}F]FDG	Esophageal	79	FD is an independent predictor of survival.
Lopci et al. [70]	[^{64}Cu]ATSM	NSCLC, head and neck	5	No significant difference of FD values at early and late assessment
Non-oncology				
Kuikka et al. [71]	[^{123}I]1β-CIT (SPECT)	Brain	39	Higher heterogeneity in females and striatal asymmetry (left to right)
Kuikka et al. [72]	[^{99m}Tc] (SPECT)	Brain	20	Lower fractal dimension in patients with dementia of frontal lobe type
Lee et al. [73]	[^{18}F]FDG	Brain	66	Higher fractal dimensions in older healthy volunteers
Venegas and Galletti [74]	[^{13}N]nitrogen	Lung	6	FD as alternative method to analyze pulmonary perfusion
Kalliokoski et al. [75]	[^{15}O]water	Muscle	15	Perfusion distribution in resting and exercising muscle
Kalliokoski et al. [76]	[^{15}O]water	Muscle	21	Perfusion distribution in resting and exercising muscle in trained and untrained muscles

Abbreviations: *m-FD*, morphologic fractal dimension; *d-FD*, density fractal dimension; *NSCLC*, non-small cell lung carcinoma; *NETs*, neuroendocrine tumors; *SPECT*, single-photon emission computed tomography

significant decrease of fractal dimension, as well as SUV values [66]. These findings were also in agreement with previous results from Dimitrakopoulou-Strauss et al. [67] in multiple myeloma during chemotherapy. Ben Bouallègue et al. [68] found that lower values of both the 2D and 3D fractal dimensions were significantly associated with higher rates of complete metabolic response in malignant lymphomas, inferring that fractal dimensions reflect, at the macroscopic level, histological feature and tumor perfusion distribution, with cellular and perfusion homogeneity being favorable factors for therapeutic response.

Tochigi et al. [69] assessed the heterogeneity of the intratumoral glucose metabolism by fractal analysis and evaluated its prognostic impact in patients with esophageal cancer. Kaplan–Meier curve showed tumors with low fractal dimension (≤ 1.95) had better survival than those with high fractal dimension values. Moreover, fractal dimension was confirmed as an independent factor for patient survival.

Finally, Lopci et al. [70] analyzed early and delayed acquisition on copper-64 diacetyl-bisN4-methylthiosemicarbazone ([^{64}Cu]ATSM) PET/CT in a small cohort of cancer patients. For fractal geometry values, the preliminary findings showed not significant difference at early and late acquisition, supporting the role of [^{64}Cu]ATSM PET/CT images for the assessment of tumor hypoxia.

Fractal Geometry in Non-oncological Nuclear Medicine

In 1997, Kuikka et al. [71] applied fractal analysis to distinguish the spatial heterogeneity of striatal dopamine reuptake sites in the living human brain, using iodine-123-labeled 2β-carbomethoxy-3β-(4-iodophenyl)tropane ([^{123}I]1β-CIT). In particular, females had a higher heterogeneity in both the left and the right striatum. Moreover, they found significant striatal asymmetry, suggesting functional hemispheric lateralization. Afterwards, the same group reported that the heterogeneity of blood flow with a fractal approach was able to differentiate dementia of the frontolobar type from control subjects [72]. Additionally, Lee et al. [73] showed heterogeneity in the cerebral glucose metabolism of healthy volunteers, expressed by fractal dimensions, was higher in older volunteers in most brain region, whereas no significant differences between male and female volunteers of the same age were found.

Venegas and Galletti [74] applied an alternative method of using fractal dimension to analyze pulmonary perfusion with PET after injection of a bolus of [^{13}N]nitrogen saline. They accounted for the irregular shape of the organ and corrected for the vertical perfusion gradient in the lung.

Other papers investigated fractal values of perfusion images with [^{15}O]water PET comparing resting *versus* exercising muscle and trained *versus* untrained subjects. However, no significant differences in perfusion distribution were observed by fractal analysis highlighting that vascular branching patterns do not majorly contribute to perfusion heterogeneity [75, 76].

In Table 1, we have summarized all nuclear medicine studies where fractal analysis was performed.

Conclusions

It remains indubitable that many factors may affect the interpretations of the computed tomography or PET images. What makes the tasks difficult is the fact that although the basic anatomy is fundamentally the same from image to image, the degree of natural dissimilarity in both normal and pathological anatomical structures is high, and clinicians will never see all possible variations no matter how long they practice and how many images they see. The need to find a new way of objectively observing, classifying, and measuring the normal and abnormal anatomical forms, and their complex dynamical changes prompted many investigators to develop computer-aided diagnosis algorithms based on fractal geometry. The fascination for the small and infinitely small has led to the illustration of details invisible to even the most acute observation of the human eye. The conception of anatomical systems as an infinite hierarchy of infinitely graduated forms implies the existence of realities invisible to the naked eye, thus highlighting new properties of organized biological matter and raising a series of new and intriguing questions. Although widely used in the physics since the beginning of the twentieth century, it is also indubitable that the concepts of *complexity*, *irregularity*, and *self-similarity* need to enter in the lexical armamentarium or be applied to the nuclear medicine.

Acknowledgments. The "Michele Rodriguez" Foundation is acknowledged for the scientific support.

Funding Information. The Italian Association for Research on Cancer (AIRC—Associazione Italiana per la Ricerca sul Cancro) provided financial support for the research with the grant no. 18923.

Compliance with Ethical Standards

Conflict of Interest

The authors declare that they have no conflict of interest.

References

1. Kane EA, Higham TE (2015) Complex systems are more than the sum of their parts: using integration to understand performance, biomechanics, and diversity. Integr Comp Biol 55:146–165
2. Grizzi F, Chiriva-Internati M (2005) The complexity of anatomical systems. Theor Biol Med Model 19:2–26
3. Simon AH (1962) The architecture of complexity. Proc Am Philos Soc 106:467–482
4. Di Ieva A, Grizzi F, Jelinek H et al (2014) Fractals in the neurosciences, part I: general principles and basic neurosciences. Neuroscientist 20:403–417
5. Noble D (2008) Claude Bernard, the first systems biologist, and the future of physiology. Exp Physiol 93:16–26
6. Sargut G, McGrath RG (2011) Learning to live with complexity. Harv Bus Rev 89(68–76):136
7. Losa GA (2009) The fractal geometry of life. Riv Biol 102:29–59

8. Losa GA (2002) Fractal morphometry of cell complexity. Riv Biol 95:239–258
9. Bianciardi G (2015) Differential diagnosis. Shape and function, fractal tools in the pathology lab. Nonlinear Dynamics Psychol Life Sci 19:437–464
10. Losa GA, Nonnenmacher TF (1996) Self-similarity and fractal irregularity in pathologic tissues. Mod Pathol 9:174–182
11. Lennon FE, Cianci GC, Cipriani NA, Hensing TA, Zhang HJ, Chen CT, Murgu SD, Vokes EE, Vannier MW, Salgia R (2015) Lung cancer—a fractal viewpoint. Nat Rev Clin Oncol 12:664–675
12. Di Ieva A, Esteban FJ, Grizzi F et al (2015) Fractals in the neurosciences, part II: clinical applications and future perspectives. Neuroscientist 21:30–43
13. Im K, Lee JM, Yoon U, Shin YW, Hong SB, Kim IY, Kwon JS, Kim SI (2006) Fractal dimension in human cortical surface: multiple regression analysis with cortical thickness, sulcal depth, and folding area. Hum Brain Mapp 27:994–1003
14. Gadde SG, Anegondi N, Bhanushali D et al (2016) Quantification of vessel density in retinal optical coherence tomography angiography images using local fractal dimension. Invest Ophthalmol Vis Sci 57:246–252
15. Noujaim SF, Berenfeld O, Kalifa J, Cerrone M, Nanthakumar K, Atienza F, Moreno J, Mironov S, Jalife J (2007) Universal scaling law of electrical turbulence in the mammalian heart. Proc Natl Acad Sci U S A 104:20985–20989
16. Goldberger AL (1991) Is the normal heartbeat chaotic or homeostatic? News Physiol Sci 6:87–91
17. Mandelbrot B (1967) How long is the coast of Britain? Statistical self-similarity and fractional dimension. Science 156(3775):636–638
18. Bancaud A, Lavelle C, Huet S, Ellenberg J (2012) A fractal model for nuclear organization: current evidence and biological implications. Nucleic Acids Res 40:8783–8792
19. Glenny RW, Robertson HT, Yamashiro S, Bassingthwaighte JB (1991) Applications of fractal analysis to physiology. J Appl Physiol 70:2351–2367
20. Liebovitch LS, Todorov AT (1996) Using fractals and nonlinear dynamics to determine the physical properties of ion channel proteins. Crit Rev Neurobiol 10:169–187
21. West BJ (2010) Fractal physiology and the fractional calculus: a perspective. Front Physiol 14:1–12
22. Cross SS (1997) Fractals in pathology. J Pathol 182:1–8
23. Smith TG Jr, Lange GD, Marks WB (1996) Fractal methods and results in cellular morphology—dimensions, lacunarity and multifractals. J Neurosci Methods 69:123–136
24. Grizzi F, Russo C, Colombo P et al (2005) Quantitative evaluation and modeling of two-dimensional neovascular network complexity: the surface fractal dimension. BMC Cancer 8:5–14
25. Havlin S, Buldyrev SV, Goldberger AL, Mantegna RN, Ossadnik SM, Peng CK, Simons M, Stanley HE (1995) Fractals in biology and medicine. Chaos, Solitons Fractals 6:171–201
26. Grizzi F, Colombo P, Taverna G, Chiriva-Internati M, Cobos E, Graziotti P, Muzzio PC, Dioguardi N (2007) Geometry of human vascular system: is it an obstacle for quantifying antiangiogenic therapies? Appl Immunohistochem Mol Morphol 15:134–139
27. Captur G, Karperien AL, Li C et al (2015) Fractal frontiers in cardiovascular magnetic resonance: towards clinical implementation. J Cardiovasc Magn Reson 7:17–80
28. Lorthois S, Cassot F (2010) Fractal analysis of vascular networks: insights from morphogenesis. J Theor Biol 262:614–633
29. Moal F, Chappard D, Wang J et al (2002) Fractal dimension can distinguish models and pharmacologic changes in liver fibrosis in rats. Hepatology 36:840–849
30. Rajkovic K, Bacic G, Ristanovic D, Milosevic NT (2014) Mathematical model of neuronal morphology: prenatal development of the human dentate nucleus. Biomed Res Int 2014:812351
31. Ristanovic D, Stefanovic BD, Puskas N (2014) Fractal analysis of dendrite morphology using modified box-counting method. Neurosci Res 84:64–67
32. Ristanovic D, Stefanovic BD, Puskas N (2014) Fractal analysis of dendrite morphology of rotated neuronal pictures: the modified box counting method. Theor Biol Forum 107:109–121
33. Tambasco M, Magliocco AM (2008) Relationship between tumor grade and computed architectural complexity in breast cancer specimens. Hum Pathol 39:740–746
34. Liebovitch LS, Toth TI (1990) Fractal activity in cell membrane ion channels. Ann N Y Acad Sci 591:375–391
35. Dioguardi N, Grizzi F, Fiamengo B, Russo C (2008) Metrically measuring liver biopsy: a chronic hepatitis B and C computer-aided morphologic description. World J Gastroenterol 14:7335–7344
36. Grizzi F, Russo C, Franceschini B, di Rocco M, Torri V, Morenghi E, Fassati LR, Dioguardi N (2006) Sampling variability of computer-aided fractal-corrected measures of liver fibrosis in needle biopsy specimens. World J Gastroenterol 12:7660–7665
37. Dioguardi N, Grizzi F, Franceschini B, Bossi P, Russo C (2006) Liver fibrosis and tissue architectural change measurement using fractal-rectified metrics and Hurst's exponent. World J Gastroenterol 12:2187–2194
38. Dioguardi N, Franceschini B, Aletti G, Russo C, Grizzi F (2003) Fractal dimension rectified meter for quantification of liver fibrosis and other irregular microscopic objects. Anal Quant Cytol Histol 25:312–320
39. Dioguardi N, Grizzi F, Bossi P, Roncalli M (1999) Fractal and spectral dimension analysis of liver fibrosis in needle biopsy specimens. Anal Quant Cytol Histol 21:262–266
40. Sedivy R (1996) Fractal tumours: their real and virtual images. Wien Klin Wochenschr 108:547–551
41. Kikuchi A, Kozuma S, Yasugi T, Taketani Y (2004) Fractal analysis of surface growth patterns in endometrioid endometrial adenocarcinoma. Gynecol Obstet Investig 58:61–67
42. Lee LH, Tambasco M, Otsuka S, Wright A, Klimowicz A, Petrillo S, Morris D, Magliocco A, Bebb DG (2014) Digital differentiation of non-small cell carcinomas of the lung by the fractal dimension of their epithelial architecture. Micron 67:125–131
43. Vasiljevic J, Reljin B, Sopta J, Mijucic V, Tulic G, Reljin I (2012) Application of multifractal analysis on microscopic images in the classification of metastatic bone disease. Biomed Microdevices 14:541–548
44. Di Ieva A, Grizzi F, Tschabitscher M et al (2010) Correlation of microvascular fractal dimension with positron emission tomography [^{11}C]-methionine uptake in glioblastoma multiforme: preliminary findings. Microvasc Res 80:267–273
45. Metze K (2013) Fractal dimension of chromatin: potential molecular diagnostic applications for cancer prognosis. Expert Rev Mol Diagn 13:719–735
46. Fudenberg G, Getz G, Meyerson M, Mirny LA (2011) High order chromatin architecture shapes the landscape of chromosomal alterations in cancer. Nat Biotechnol 29:1109–1113
47. Misteli T (2010) Higher-order genome organization in human disease. Cold Spring Harb Perspect Biol 2(8):a000794
48. Irinopoulou T, Rigaut JP, Benson MC (1993) Toward objective prognostic grading of prostatic carcinoma using image analysis. Anal Quant Cytol Histol 15:341–344
49. Streba CT, Pirici D, Vere CC, Mogoantă L, Comănescu V, Rogoveanu I (2011) Fractal analysis differentiation of nuclear and vascular patterns in hepatocellular carcinomas and hepatic metastasis. Romanian J Morphol Embryol 52:845–854
50. Strauss LG, Conti PS (1991) The applications of PET in clinical oncology. J Nucl Med 32:623–648
51. Barrington SF, Mikhaeel NG, Kostakoglu L, Meignan M, Hutchings M, Müeller SP, Schwartz LH, Zucca E, Fisher RI, Trotman J, Hoekstra OS, Hicks RJ, O'Doherty MJ, Hustinx R, Biggi A, Cheson BD (2014) Role of imaging in the staging and response assessment of lymphoma: consensus of the International Conference on Malignant Lymphomas Imaging Working Group. J Clin Oncol 32:3048–3058
52. Dimitrakopoulou-Strauss A (2015) PET-based molecular imaging in personalized oncology: potential of the assessment of therapeutic outcome. Future Oncol 11:1083–1091
53. Mijnhout GS, Hoekstra OS, van Tulder MW, Teule GJJ, Devill WLJM (2001) Systematic review of the diagnostic accuracy of (18)F-fluorodeoxyglucose positron emission tomography in melanoma patients. Cancer 91:1530–1542
54. Kessler LG, Barnhart HX, Buckler AJ, Choudhury KR, Kondratovich MV, Toledano A, Guimaraes AR, Filice R, Zhang Z, Sullivan DC, QIBA Terminology Working Group (2015) The emerging science of quantitative imaging biomarkers terminology and definitions for scientific studies and regulatory submissions. Stat Methods Med Res 24:9–26

55. Michallek F, Dewey M (2014) Fractal analysis in radiological and nuclear medicine perfusion imaging: a systematic review. Eur Radiol 24:60–69
56. Miwa K, Inubushi M, Wagatsuma K, Nagao M, Murata T, Koyama M, Koizumi M, Sasaki M (2014) FDG uptake heterogeneity evaluated by fractal analysis improves the differential diagnosis of pulmonary nodules. Eur J Radiol 83:715–719
57. Dimitrakopoulou-Strauss A, Georgoulias V, Eisenhut M, Herth F, Koukouraki S, Mäcke HR, Haberkorn U, Strauss LG (2006) Quantitative assessment of SSTR2 expression in patients with non-small cell lung cancer using ^{68}Ga-DOTATOC PET and comparison with ^{18}F-FDG PET. Eur J Nucl Med Mol Imaging 33:823–830
58. Dimitrakopoulou-Strauss A, Strauss LG, Burger C (2001) Quantitative PET studies in pretreated melanoma patients: a comparison of 6-[^{18}F]fluoro-L-dopa with 18F-FDG and ^{15}O-water using compartment and noncompartment analysis. J Nucl Med 42:248–256
59. Breki CM, Dimitrakopoulou-Strauss A, Hassel J, Theoharis T, Sachpekidis C, Pan L, Provata A (2016) Fractal and multifractal analysis of PET/CT images of metastatic melanoma before and after treatment with ipilimumab. EJNMMI Res 6:61
60. Dimitrakopoulou-Strauss A, Strauss LG, Schwarzbach M, Burger C, Heichel T, Willeke F, Mechtersheimer G, Lehnert T (2001) Dynamic PET ^{18}F-FDG studies in patients with primary and recurrent soft-tissue sarcomas: impact on diagnosis and correlation with grading. J Nucl Med 42:713–720
61. Okazumi S, Dimitrakopoulou-Strauss A, Schwarzbach MH, Strauss LG (2009) Quantitative, dynamic ^{18}F-FDG-PET for the evaluation of soft tissue sarcomas: relation to differential diagnosis, tumor grading and prediction of prognosis. Hell J Nucl Med 12:223–228
62. Dimitrakopoulou-Strauss A, Strauss LG, Burger C, Rühl A, Irngartinger G, Stremmel W, Rudi J (2004) Prognostic aspects of ^{18}F-FDG PET kinetics in patients with metastatic colorectal carcinoma receiving FOLFOX chemotherapy. J Nucl Med 45:1480–1487
63. Koukouraki S, Strauss LG, Georgoulias V, Eisenhut M, Haberkorn U, Dimitrakopoulou-Strauss A (2006) Comparison of the pharmacokinetics of 68Ga-DOTATOC and [^{18}F]FDG in patients with metastatic neuroendocrine tumours scheduled for 90Y-DOTATOC therapy. Eur J Nucl Med Mol Imaging 33:1115–1122
64. Sachpekidis C, Kopka K, Eder M et al (2016) ^{68}Ga-PSMA-11 dynamic PET/CT imaging in primary prostate cancer. Clin Nucl Med 41:e473–e479
65. Sachpekidis C, Baumer P, Kopka K et al (2018) ^{68}Ga-PSMA PET/CT in the evaluation of bone metastases in prostate cancer. Eur J Nucl Med Mol Imaging 45:904–912. https://doi.org/10.1007/s00259-018-3936-0
66. Sachpekidis C, Hillengass J, Goldschmidt H, Wagner B, Haberkorn U, Kopka K, Dimitrakopoulou-Strauss A (2017) Treatment response evaluation with ^{18}F-FDG PET/CT and ^{18}F-NaF PET/CT in multiple myeloma patients undergoing high-dose chemotherapy and autologous stem cell transplantation. Eur J Nucl Med Mol Imaging 44:50–62
67. Dimitrakopoulou-Strauss A, Hoffmann M, Bergner R, Uppenkamp M, Haberkorn U, Strauss LG (2009) Prediction of progression-free survival in patients with multiple myeloma following anthracycline-based chemotherapy based on dynamic FDG-PET. Clin Nucl Med 34:576–584
68. Ben Bouallegue F, Tabaa YA, Kafrouni M et al (2017) Association between textural and morphological tumor indices on baseline PET-CT and early metabolic response on interim PET-CT in bulky malignant lymphomas. Med Phys 44:4608–4619
69. Tochigi T, Shuto K, Kono T, Ohira G, Tohma T, Gunji H, Hayano K, Narushima K, Fujishiro T, Hanaoka T, Akutsu Y, Okazumi S, Matsubara H (2017) Heterogeneity of glucose metabolism in esophageal cancer measured by fractal analysis of fluorodeoxyglucose positron emission tomography image: correlation between metabolic heterogeneity and survival. Dig Surg 34:186–191
70. Lopci E, Grizzi F, Russo C, Toschi L, Grassi I, Cicoria G, Lodi F, Mattioli S, Fanti S (2017) Early and delayed evaluation of solid tumours with ^{64}Cu-ATSM PET/CT: a pilot study on semiquantitative and computer-aided fractal geometry analysis. Nucl Med Commun 38:340–346
71. Kuikka JT, Tiihonen J, Karhu J et al (1997) Fractal analysis of striatal dopamine re-uptake sites. Eur J Nucl Med Mol Imaging 24:1085–1090
72. Kuikka JT, Hartikainen P (2000) Heterogeneity of cerebral blood flow: a fractal approach. Nuklearmedizin 39:37–42
73. Lee JS, Lee DS, Park KS, Chung JK, Lee MC (2004) Changes in the heterogeneity of cerebral glucose metabolism with healthy aging: quantitative assessment by fractal analysis. J Neuroimaging 14:350–356
74. Venegas JG, Galletti GG (2000) Low-pass filtering, a new method of fractal analysis: application to PET images of pulmonary blood flow. J Appl Physiol 88:1365–1373
75. Kalliokoski KK, Kuusela TA, Nuutila P, Tolvanen T, Oikonen V, Teräs M, Takala TES, Knuuti J (2001) Perfusion heterogeneity in human skeletal muscle: fractal analysis of PET data. Eur J Nucl Med Mol Imaging 28:450–456
76. Kalliokoski KK, Kuusela TA, Laaksonen MS, Knuuti J, Nuutila P (2003) Muscle fractal vascular branching pattern and microvascular perfusion heterogeneity in endurance-trained and untrained men. J Physiol 546:529–535